Semiconductor Physics, Quantum Electronics & Optoelectronics, 2023. V. 26, No 4. P. 424-431.

Hetero- and low-dimensional structures

Impedance of nanocomposite SiO_2(Si)&Fe_xO_y(Fe) thin films containing Si and Fe nanoinclusions

A.A. Evtukh, A.Yu. Kizjak, S.V. Antonin*, O.L. Bratus

V. Lashkaryov Institute of Semiconductor Physics, NAS of Ukraine
41, prosp. Nauky, 03680 Kyiv, Ukraine
**Corresponding author e-mail: antoninsv@gmail.com*

Abstract. In this study, electrical properties at alternating current of the nanocomposite films containing silicon and iron inclusions in amorphous SiO_x matrix are presented. The composite SiO_2(Si)&Fe_xO_y(Fe) films were obtained using the ion-plasma co-sputtering of Si and Fe targets in oxygen containing atmosphere (Ar + O_2) followed by temperature annealing. It was revealed the predominance of the inductive contribution over the capacitive one in the reactive part of the admittance (impedance) at low frequencies (f < 1 MHz) both after annealing in air and nitrogen atmosphere. The frequency dependences of the admittance after heat treatment in air have the minima that shift to the region of high frequencies with increasing the annealing temperature. In the case of low-frequency dependence, the phase shift angle passes into the region of positive values, which indicates the predominance of the inductive contribution to the admittance at these frequencies. The dependence of the conductivity real part at the alternating current frequency does not change significantly up to ~20 kHz. Starting from the frequency higher than ~20 KHz and up to ~1 MHz, the exponent in the frequency dependence of the conductivity lies within the limits $m \sim 0.49…0.52$.

Keywords: nanocomposite films, Si nanoclusters, Fe nanoinclusions, oxide matrix, electrical properties, alternating current, impedance.

https://doi.org/10.15407/spqeo26.04.424
PACS 62.25.De, 73.61.-r, 81.07.-b, 81.15.-z

Manuscript received 03.10.23; revised version received 26.10.23; accepted for publication 22.11.23; published online 05.12.23.

1. Introduction

Properties of films in which nanocrystalline inclusions are located in the dielectric matrix are intensively studied in connection with the possibility to create various electronic and optoelectronic devices based on them (single-electron transistors, resonance tunnel diodes, *etc.*). Operation of these devices is related to the fact that they are based on the unique properties of these films, namely, on the low-dimensional effects that define these properties. Since one of the most common modern technologies in electronics is silicon, for which most of the technological processes are well developed, it is natural to use its capabilities to obtain structures with nanoinclusions. In this case, a film of silicon dioxide (SiO_2) can be used as a dielectric matrix, and silicon and/or metal nanoclusters can be used as the nanoinclusions.

One of the problems of modern integrated micro-electronics is to develop technology for creating the elec-trotechnical elements that play the role of inductances and capacitances that have micrometer or submicrometer sizes and can be used in hybrid integrated circuits (HIC) and conventional integrated circuits (IC) as well as for other applications. The main methods of creating such elements with inductive resistance are their imitation by using various circuit techniques or formation of the film Archimedean spirals [1]. Due to the size limitation of ICs, the inductance value of these flat "coils" is usually less than 15 μH/cm^2 [1]. Imitation of inductances by using the circuit engineering methods also leads to irrational use of the chip area and relatively small values of equivalent inductances.

In this regard, there is an urgent task to form, in the framework of technology for manufacturing silicon ICs and HIC, small-sized turn-free planar elements with inductance properties based on nanoheterogeneous, including nanocomposite metal-non-metal materials. The "negative capacitance" effect described in such systems [1–9] directly indicates formation of an inductive contribution to the reactive part of the impedance in them under certain conditions.

In recent years, special attention has been paid to creation of nano- and microstructures that under certain conditions provide a positive phase shift between electric current and voltage, which is called the "negative capacitance" effect. This effect is equivalent to the predominance of the inductive component over the capacitive one in the reactive part of the impedance. Previously, it was observed in *p-n* junctions [1, 2] and granular nanocomposites [4–16], reaching several tens of microhenries per diode. Although this type of micro-inductances fully fits into the principles of planar silicon technology, the values of operating parameters provided by them are not too large. In addition, the occurrence of inductive impedance in the *p-n* junction is possible only after additional exposure to hard radiation.

Nanocomposite metal-semiconductor-dielectric materials with the effect of "negative capacitance" [4–8, 10–16], where Al_2O_3, CaF_2 acted as the dielectric phase and the own oxides of the metal nanoparticles incorporated into the dielectric matrix acted as the semiconductor phase. They look more promising for the development of new types of turnless inductances with controlled parameters for their use in IC and HIC. As experimentally shown in the work [15], the values of specific "effective inductances" in granular nanocomposites containing oxidized nanoparticles of alloys based on iron and cobalt in dielectric matrices reached acceptable values (up to 20 μH/μm^3). However, these films are not very well compatible with planar silicon technology due to non-standard dielectric phases. In this sense, it is more promising to use silicon oxide as a dielectric matrix that is included into all planar silicon technologies for obtaining the integrated circuits [17].

On the other hand, nanocomposite films containing nanoinclusions of silicon nanoparticles and metals as well as their oxides in an amorphous matrix are promising to be used as electromagnetic radiation absorbers. Currently, a wide variety of microwave-absorbing materials is intensively researched to create the good microwave absorber [18–23]. Among the various microwave absorbing materials, ferrites such as ferrospinels and hexaferrites have attracted considerable research interest due to their high magnetic losses. Currently, a large number of ferrite microwave absorbers have been developed, including $ZnFe_2O_4$, $BaFe_{12-x}Al_xO_{19}$ (x = 0.1…1.2), and $Ce(FeTi)O_x$, which have great potential in the field of microwave absorption due to their excellent magnetic and dielectric properties. Single-component microwave absorbing materials are difficult to meet the requirements of ideal microwave absorbers. Thus, the main direction of research has become the full use of the advantages of various materials for preparation of additional multi-component materials that absorb microwaves. Various $ZnFe_2O_4$ composites, namely: core-shell $ZnFe_2O_4$/polypyrrole nanoparticles, Fe/$ZnFe_2O_4$ composites, $ZnFe_2O_4$/C composites, *etc*., have been prepared up to now. In addition, the combination of nanoparticle fillers and polymer matrix is also an idea for preparation of composite materials for microwave absorption.

This paper presents the results of studies of the alternating current electrical characteristics of SiO_xFe_y and $SiO_x(Si)\&Fe_xO_y(Fe)$ nanocomposite films containing silicon and iron nanoinclusions in an amorphous silicon oxide matrix. Nanocomposite $SiO_x(Si)\&Fe_xO_y(Fe)$ films resulted from high temperature annealing of the as-deposited SiO_xFe_y films. Being based on the impedance analysis, it was demonstrated that the obtained nanocomposite films containing silicon nanoparticles and iron inclusions embedded into amorphous SiO_x matrix may have the predominant capacitive or inductive component in the total resistance at alternating voltage depending on the frequency and nature of the composite film.

2. Experimental

2.1. Sample preparation

2.1.1. Ion-plasma film deposition technology

To obtain thin films of high purity, the partial pressure of chemically active gases must be low, and the sputtering speed must be high. These conditions are provided by using the method of gas discharge plasma sputtering at low pressure (ion-plasma technology). The vacuum sputtering installation is designed for deposition of metal, semiconductor and dielectric films by using the method of ion-plasma (for dielectrics, reactive) sputtering.

The main feature of the ion-plasma sputtering method is that the independent gas discharge acts in the space between the target electrode (with the sputtering material applied to it) and the substrate. This type of discharge is characterized by the presence of a special source of electrons in the form of the thermocathode, the emission current of which reaches 10…20 A, low operating voltages (tens of volts) and the higher density of electron-ion plasma. The subcapsular space is filled with neutral gas, at the low pressure $P = 10^{-3}…10^{-4}$ Torr. The voltage of 50 to 80 V is applied between the anode and cathode. The sputtered material in the form of the plate (target) is placed as third electrode between anode and cathode. A negative bias of 1 to 3 kV relative to the anode is applied to it, and the grounded substrate is placed opposite.

When sputtering the dielectric films, the problem arises related to accumulation of the positive charge on the target, which prevents further ion bombardment. This problem is overcome using the so-called high-frequency ion-plasma sputtering. In this case, a high-frequency alternating voltage (about 15 MHz) with an amplitude slightly higher than the constant voltage is applied to the target simultaneously with the constant negative voltage. During most part of the period, the resulting voltage is negative; at the same time, the usual process of atomization of the target takes place, and the positive charge is accumulated on it. However, during a small part of the period, the resulting voltage is positive; at the same time, the target is bombarded with electrons from the plasma, *i.e*. no sputtering occurs, so the accumulated positive charge is compensated.

The option of reactive (chemical) ion-plasma sputtering opens up the possibility to prepare oxides, nitrides and other compounds. The advantages of the ion-plasma method, in comparison with the cathode and magnetron sputtering methods, are higher speed of sputtering and greater flexibility of the process (possibility of ion cleaning, possibility of disconnecting the working circuit without interrupting the discharge, *etc*). In addition, the quality of films is affected by higher vacuum.

As a result of the high energy inherent to the atoms of sputtered material and the cleaning effect of gas ions on the substrate, the obtained coatings have high adhesion. It is 1–2 orders of magnitude higher than that during thermal evaporation.

To improve the adhesion of deposited film to the substrate, the heater was installed in the volume of the chamber, which allows to control the temperature of the substrate within the range from 50 to 300 °C. Temperature control was carried out with the thermocouple that was connected at one end to the heater, and then through vacuum contacts in the chamber, it had its output to the millivoltmeter. To obtain the high vacuum and reduce the content of residual gases, the nitrogen trap is installed in the operation chamber equipped with the diffusion pump, to which liquid nitrogen from the Dewar vessel was supplied through the pipeline.

The main characteristic of the effectiveness of the sputtering process is the sputtering coefficient K_p, which is defined by the ratio of the number of knocked-out atoms N_{at} to the number of ions N_{ion} bombarding the target:

$$K_p = \frac{N_{at}}{N_{ion}}. \tag{1}$$

In essence, the sputtering coefficient is the average number of the target atoms knocked out by one ion. The sputtering coefficient depends on the ion energy E_i, their mass (type of operation gas), material of the target, and to some extent on its temperature and surface condition, bombardment angle, gas pressure (provided that the pressure does not exceed the limits at which the gas-discharge plasma extinguishes). The dependence of the sputtering coefficient on the ion energy is non-monotonic. At first, at relatively low energies (less than 100 KeV), K_p increases with increasing ion energy, and this dependence is practically linear. Then the growth of K_p slows down, the curve $K_p = f(E_i)$ reaches saturation, and for some materials there is even the decrease in the sputtering coefficient. Qualitatively, the nature of this dependence can be explained as follows. At low energies, the efficiency of the sputtering process, characterized by the sputtering coefficient, increases with the growth of the ion energy, since this leads to the increase in the momentum transferred by the ion to the target atom, and therefore to the increase in the probability of knocking it out from its node. If the energy of the ion exceeds the certain value $E_{i\max}$, then the process of ion implantation becomes more probable. This means that ions accelerated to high energies quickly penetrate the near-surface layer of the target, losing their energy due to knocking out target atoms from their nodes. However, the process of knocking out atoms takes place already at the certain depth from the surface of the target, so the significant part of the knocked-out atoms cannot pass from the target to the vapor-gas phase. As a result, the sputtering coefficient decreases with increasing the ion energy (or remains constant).

The dependence $K_p = f(E_i)$ is quite well described by the expression

$$K_p = \frac{K_0 N_2 \pi a^2}{F E_s} \cdot \frac{\sqrt{\dfrac{E_i}{E_{i\max}}}}{1+\dfrac{E_i}{E_{i\max}}}, \tag{2}$$

where the coefficient K_0 depends on the charges of the nuclei of the bombarding ion Z_1 and the target atom Z_2 and changes periodically with the change of Z_2; N_2 is the concentration of target atoms; E_s is the sublimation energy of the target material. The normalizing coefficient F is determined by the value $E_{i\max}$:

$$F = \frac{0.3}{E_{i\max}}, \tag{3}$$

The value of a in the formula (2) represents the radius of shielding of the charge of the nucleus by the electrons of the atomic shell:

$$a = \frac{4.7\cdot 10^{-9}}{\left(Z_1^{2/3}+Z_2^{2/3}\right)^{1/2}}(\text{cm}). \tag{4}$$

The dependence of sputtering coefficient on the mass of ions in the operation gas m_1 and atoms of the target m_2 is described by the expression

$$K_p = k\,\frac{m_1\cdot m_2}{\lambda(m_1+m_2)}E_i, \tag{5}$$

where k is the coefficient that characterizes the physical state of the target and is determined experimentally; λ is the free path length of ions in the target, which depends on the concentration of target atoms.

The increase in the pressure of the operation gas in the chamber increases the probability of the sputtering atoms colliding with the molecules of the operation gas, as a result of which some of the atoms are scattered in the volume or, having bounced off the molecules of the operation gas, are returned to the target. Therefore, the increase in the pressure leads to the decrease in the sputtering coefficient. Backscattering has the particularly significant effect on the value of K_p, if the mass of sputtering atoms is less than the mass of molecules in the operation gas.

The advantages of the ion sputtering method are as follows: (*i*) the large area of the target that is sputtered, which allows one to obtain the films of uniform thickness on large substrates and ensures the effective implementation of the group processing method; (*ii*) the target is the long irreplaceable source of material that facilitates automation and increases the uniformity of the process;

(*iii*) high adhesion of the film to the substrate is ensured due to the high energy of atoms that condense; (*iv*) deposition of the films from refractory metals occurs without overheating of the vacuum chamber; (*v*) deposition of the oxide, nitride and other films, including the doped ones, is possible as a result of chemical reactions of the atoms belonging to the sputtered material with the gases introduced into the chamber; (*vi*) oxidation by using plasma anodization can be carried out; (*vii*) organic films and the dielectrics can be obtained.

To obtain SiO_x films with different amounts of excess silicon and iron, we have developed the technological conditions for obtaining the SiO_x films with different amounts of excess silicon [24] or silicon and iron by ion-plasma sputtering. In the process of the ion-plasma deposition of SiO_x films with different contents of silicon and iron, sputtering of the combined silicon and iron target in the environment of argon and oxygen was carried out. The change in the ratio of reaction gases O_2/Ar in the chamber leads to the different proportion of oxidized silicon and iron atoms and the different content of excess silicon and iron in the SiO_x films. In the process of ion-plasma sputtering, when depositing the SiO_xFe_y film, silicon and iron atoms are oxidized (knocked out by ions from the combined silicon-iron target), and the degree of atom oxidation depends on the gas ratio of oxygen and argon supplied to the chamber during the sputtering process. The parameters of the deposition process were as follows: gas pressure in the chamber $P = 5\cdot10^{-4}…8\cdot10^{-4}$ Torr ($P = 6.7\cdot10^{-3}…1\cdot10^{-2}$ Pa), substrate temperature T = 100…120 °C, cathode heating current I_K = 150 A, anode voltage U_A = 50 V, anode current I_a = 11 A, voltage on the target U_m = 0.9…1.1 kV, target current I_m = 0.6…0.7 mA. The ratio of the areas of silicon and iron parts in the target Si/Fe = 0.75/0.25 = 3.

To study the electrical characteristics of SiO_xFe_y and SiO_x(Si)&Fe_xO_y(Fe) films, metal-insulator-semiconductor (MIS) structures were formed on *p*-type silicon substrates with the resistivity of 10 Ohm·cm and orientation (100). The circular Al electrodes with the thickness of 0.5 μm and the area of $S = 7.85\cdot10^{-3}$ cm^2 were deposited using the magnetron sputtering through the mask on the films deposited on the front sides of the Si substrates. Silicon-enriched SiO_xFe_y and SiO_x(Si)&Fe_xO_y(Fe) films containing nanoinclusions of silicon and iron were used as the dielectrics. The SiO_x(Si)&Fe_xO_y(Fe) film was formed in the process of high-temperature T = 1100 °C annealing in the nitrogen atmosphere of the as-deposited SiO_xFe_y film [23].

2.2. Measurements

The impedance measurements (AC method) were used to determine the capacitive and inductive properties of nanocomposite films containing silicon and metal (Fe) nanoclusters. The measurements were performed with Agilant 4294A semiconductor parameter analyzer within the frequency range of testing signal 10 Hz…6 MHz. The amplitude of testing signal was 20 mV.

To determine the capacitance of the integrated impedance measured using the AC method, there are two impedance models: the series and parallel ones. In the series model, the full impedance is expressed by the combined values of the series capacitance (C_s) and the consecutive resistor. In the parallel model, the full impedance or total complex conductivity (admittance) is expressed by two related values: parallel capacitance (C_p) and parallel conductivity. The choice of the corresponding mode of the measuring circuit is important for accurate analysis of the interrelations between the parasitic and physical parameters. One of the reasons is that the calculated values of *C*, *L*, *R* and other parameters are different depending on the mode of the measuring circuit. To define the mode of measurement scheme suitable for the measurement and analysis, we used criteria given in [25]. In our case, the series connection of the *C*, *L*, *R* components in the equivalent circuit was realized.

3. Results and discussion

3.1. Admittance of SiO_xFe_y films

The frequency dependences of the admittance and the phase shift angle of the initial and annealed in air at different temperatures SiO_x(Fe) films are shown in Fig. 1. As can be seen, the annealing significantly affects the shape of the curves σ(*f*) and θ(*f*). In particular, on the dependences of the admittance σ(*f*) after heat treatment

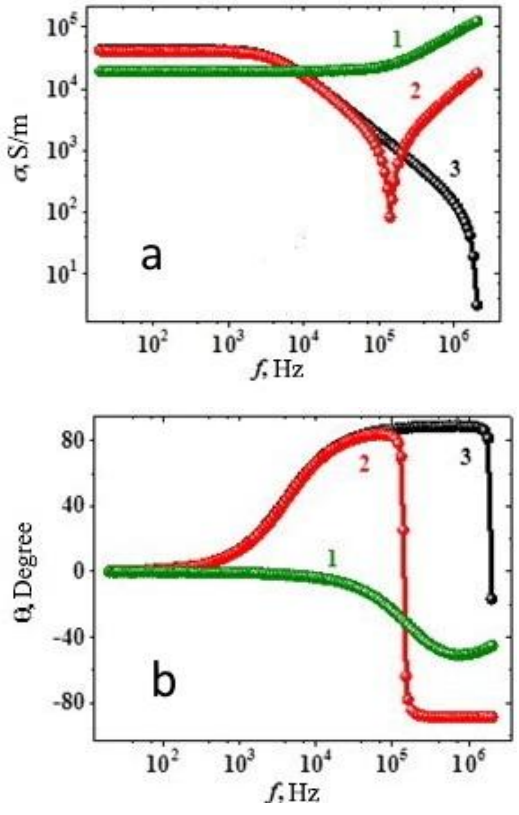

Fig. 1. Frequency dependences of total admittance σ(*f*) (a) and phase shift angle θ(*f*) (b) for composite SiO_xFe_y thin films, measured after annealing in air at different temperatures: *1* – before annealing, *2* – T_a = 673 K, *3* – T_a = 773 K.

there are minima, which shift to the region of high frequencies with increasing the annealing temperature. In this case, the low-frequency dependence θ(*f*) passes into the region of positive values, which indicates predominance of the inductive contribution to the admittance at frequencies to the left of the minimum on the curves σ(*f*). This behavior of the dependences σ(*f*) and θ(*f*) may be caused by the fact that the admittance of annealed samples with SiO_xFe_y film can be presented by equivalent circuits with the series connection of active and reactive contributions to the impedance. This is evidenced, in particular, by a decrease in the inductive contribution to the admittance with increasing frequency to the left of the minimum in σ(*f*) (since $\sigma_L \sim 1/f \cdot L$), and an increase in the capacitive contribution with frequency at high its values to the right of the minimum in σ(*f*) (since $\sigma_C \sim fC$) (Fig. 1a).

3.2. Impedance of SiO_2(Si)&Fe_xO_y(Fe) films annealed at T = 1100 °C in N_2 atmosphere

The silicon nanocrystals are formed in the silicon enriched SiO_xFe_y film during high temperature annealing. The results of the impedance measurements show that there is a significant dependence of the resistance on the frequency. To specify this dependence, the conductivity on frequency curves is shown in Fig. 2. As can be seen, the conductivity is practically independent on the frequency for the regions 1 and 2 up to ~20 KHz (region 1 corresponds to voltages from –1 V to –4 V, region 2 corresponds to voltages from 1 to 4 V). Starting with the frequency higher than ~20 KHz and up to ~ 6 MHz, the power dependence of the conductivity $G \sim f^m$, where $m \simeq 0.49\ldots0.52$ is observed. The obtained *m*-value is close to the prediction of the well-known Mott model of the hopping alternating current conductivity, which gives $m \approx 0.8$ [26]. The conductivity in this area is defined by the properties of the film. At the frequencies higher than 6 MHz, the conductivity begins to decrease.

Let's consider the reactive part of the admittance. The capacitance on voltage dependences with frequency as a parameter are presented in Fig. 3a.

Based on the results shown in Fig. 3, the capacitance on the frequency of the alternating signal dependences are shown in Fig. 4a. As can be seen, the frequency dependence of C_s is significant. In addition, there is the significant nonlinearity C_s on the frequency dependence within the range 20 KHz to 5 MHz. This difference of C_s on the frequency and its nonlinearity confirm that the series component connection in equivalent circuit better suits for the structures with SiO_2(Si)&Fe_xO_y(Fe) film.

The inductance on voltage dependences with the frequency as a parameter are shown in Fig. 3b. As can be seen, there is a significant dependence on the frequency, especially in the low frequency region. The inductance slightly change in the low frequency region (to the frequency of ~20 KHz), and then it decreases (Fig. 4b). Being based on the obtained results, it is possible to evaluate which type of imagine part of the impedance

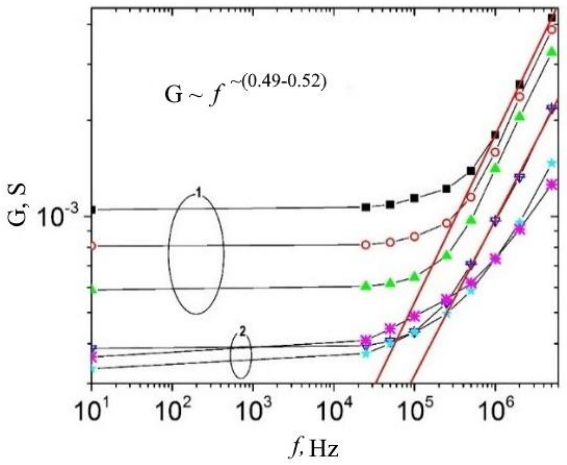

Fig. 2. Conductivity on frequency dependences of the structure with SiO_2(Si)&Fe_xO_y(Fe) film annealed at T = 1100 °C in N_2 atmosphere.

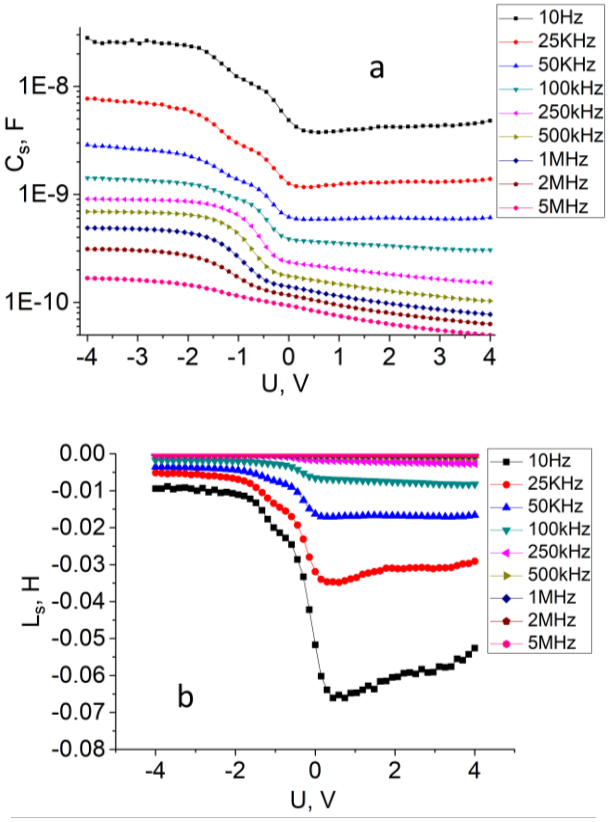

Fig. 3. Capacitance (a) and inductance (b) on voltage dependences for the structures with SiO_2(Si)&Fe_xO_y(Fe) film.

(capacitive or inductive) dominates. The reactive resistances (*X*) on the frequency dependences are shown in Fig. 5. The reactive resistance includes inductive and capacitive parts. As can be seen, the inductive component of the reactive resistance is observed till frequency of 1 MHz in the structures with SiO_2(Si)&Fe_xO_y(Fe) film, then the capacitive component dominates.

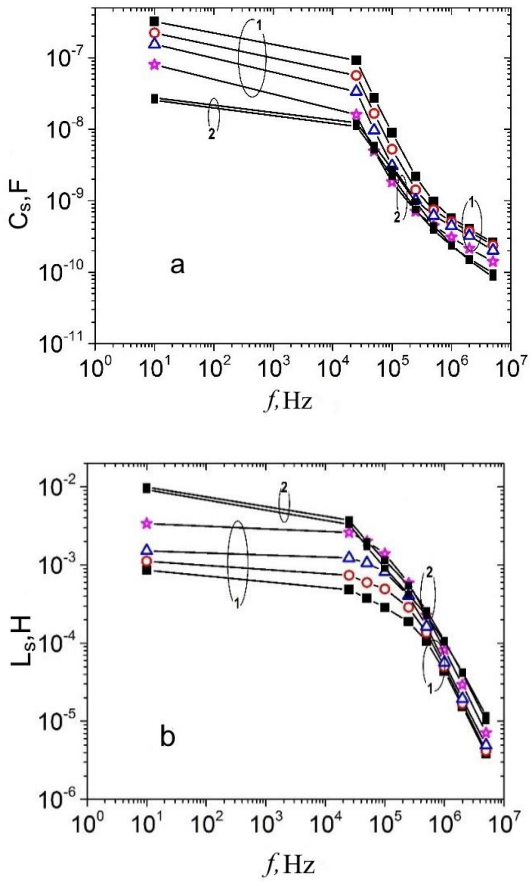

Fig. 4. Capacitance (a) and inductance (b) on the frequency dependences for the structures with SiO_2(Si)&Fe_xO_y(Fe) film.

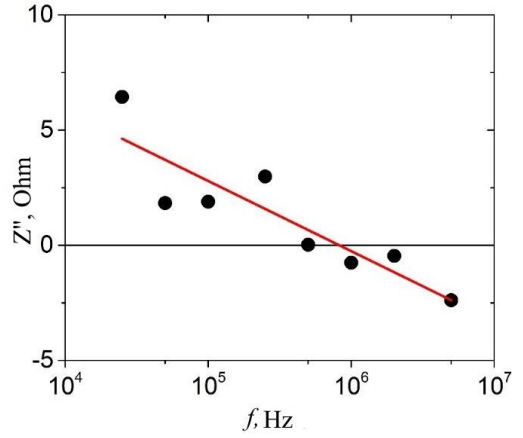

Fig. 5. Reactive part of the impedance on the frequency dependence for the structures with SiO_2(Si)&Fe_xO_y(Fe) film.

Thus, it can be concluded that the obtained structures based on SiO_x thin films with iron inclusions and excess silicon may have a predominant capacitive or inductive component in the total resistance at alternating voltage depending on the frequency and nature of the composite film, in particular, the type of metal nanoinclusion in the oxide matrix.

4. Conclusions

Being based on our measurements and analysis of electrical properties inherent to the composite films containing silicon and iron inclusions in amorphous oxide matrix, it has been shown that the dependence of the conductivity on the alternating current frequency does not change significantly up to ~20 kHz. Starting from the frequency higher than ~20 KHz and up to ~1 MHz, the exponent in the dependence of conductivity is $m \sim 0.49…0.52$. The annealing of the as-deposited SiO_xFe_y films at the temperatures from the range 773 up to 873 K in air causes predominance of inductive contribution over the capacitive one in the reactive part of the admittance at low frequencies. The frequency dependences of the admittance after heat treatment in air have the minima that shift to the region of high frequencies with increasing the annealing temperature. In this case, the low-frequency dependence of the phase shift angle passes into the region of positive values, which indicates predominance of the inductive contribution to the admittance at these frequencies. Nanocomposite SiO_2(Si)&Fe_xO_y(Fe) films formed in the course of high temperature annealing of initial SiO_xFe_y films in nitrogen also demonstrate predominance of the inductive contribution over the capacitive one in the reactive part of the impedance at frequencies below 1 MHz.

Acknowledgements

This research was supported by the project "Development of nanocomposite material technology for highly efficient absorption of electromagnetic radiation" of the National Research Foundation of Ukraine (No. 2022.01/0066).

References

1. Poklonski N.A., Shpakovski S.V., Gorbachuk N.I., Lastovskii S.B. Negative capacitance (impedance of the inductive type) of silicon p^+-n junctions irradiated with fast electrons. *Semiconductors.* 2006. **40b**, No 7. P. 803–807. https://doi.org/10.1134/S1063782606070128.
2. Partenskii J. Negative capacitance and instability at electrified interfaces: Lessons from the study of membrane capacitors. *Condens. Matter Phys.* 2005. **8**, No 2. P. 397. https://doi.org/10.5488/CMP.8.2.397.
3. Bratus' O., Evtukh A., Kaganovich E. *et al.* Charge storage characteristics of gold nanoparticles embedded in alumina matrix. *SPQEO.* 2009. **12**. P. 53–56. https://doi.org/10.15407/spqeo12.01.053.
4. Kwok H.L. Modeling negative capacitance effect in organic polymers. *Solid-State Electron.* 2003. **47**, No 6. P. 1089–1093. https://doi.org/10.1016/S0038-1101(02)00471-9.
5. Parravicini G.B., Stella A., Ungureanu M.C., Kofman R. Low-frequency negative capacitance effect in systems of metallic nanoparticles

embedded in dielectric matrix. *Appl. Phys. Lett.* 2004. **85**, No 2. P. 302–304. https://doi.org/10.1063/1.1772872.
6. Saad A.M., Mazanik A.V., Kalinin Yu.E. *et al.* Structure and electrical properties of CoFeZr-aluminium oxide nanocomposite films. *Rev. Adv. Mater. Sci*. 2004. **8**, No 2. P. 152–157.
7. Saad A.M., Andrievsky B., Fedotov A. *et al.* AC and DC carrier transport in $(FeCoZr)_x(Al_2O_3)_{1-x}$ nanocomposite films for spintronic applications. *Proc. SEMINANO.* Budapest, Hungary, September 10-12, 2005. P. 321–324.
8. Ershov M., Liu H.C., Li L. *et al.* Negative capacitance effect in semiconductor devices. *IEEE Trans. Electron. Devices.* 1998. **45**, No 10. P. 2196–2203. https://doi.org/10.1109/16.725254.
9. Evtukh A., Bratus' O., Ilchenko V. *et al.* Capacitive properties of MIS structures with SiO_x and $Si_xO_yN_z$ films containing Si nanoclusters. *JNanoR.* 2016. **39**. P. 162–168. https://doi.org/10.4028/ www.scientific.net/ JNanoR.39.162.
10. Fedotova J.A. $FeCoZr–Al_2O_3$ granular nanocomposite films with tailored structural, electric, magnetotransport and magnetic Properties. In: *Advances in Nanoscale Magnetism*, Aktas B., Mikailov F. (Eds), *Springer Proceedings in Physics*, Springer, Berlin, Heidelberg, 2009. **122**. P. 231–267. https://doi.org/10.1007/978-3-540-69882-1_13.
11. Saad A.M., Fedotov A.K., Svito I.A. *et al.* Impedance and magnetization of CoFeZr nanoclusters embedded into alumina matrix. *J. Alloys Compd*. 2006. **423**, No 1-2. P. 176–180. https://doi.org/10.1016/j.jallcom.2005.12.115.
12. Fedotova J., Saad A., Fedotova V. *et al.* Influence of oxygen and nitrogen on impedance and magnetoimpedance of soft magnetic CoFeZr nanoparticles embedded in alumina matrix. *2009 9th IEEE Conference on Nanotechnology (IEEE-NANO)*, Genoa, Italy, 2009. P. 651−654.
14. Żukowski P., Kołtunowicz T., Partyka J., Fedotova Yu.A., Larkin A.V. Hopping conductivity of metal-dielectric nanocomposites produced by means of magnetron sputtering with the application of oxygen and argon ions. *Vacuum.* 2009. **83**. P. 280–283. https://doi.org/10.1016/j.vacuum.2009.01.082.
15. Koltunowicz T.N., Fedotova P., Zhukowski J.A., Larkin A.V. Inductive-type properties of $(Co_{45}Fe_{45}Zr_{10})_x(Al_2O_3)_{100-x}$ nanocomposites produced by the ion-beam sputtering in the argon and oxygen ambient. *J. Nano- Electron. Phys.* 2012. **4**, No 1. P. 01002.
16. Larkin A.V., Fedotov A.K., Fedotova J.A. *et al.* Temperature and frequency dependences of real part of impedance in the FeCoZr-doped PZT nanogranular composites. *Mater. Sci. – Poland.* 2012. **30**, No 2. P. 75–81. https://doi.org/10.2478/s13536-012-0015-2.
17. Fedotova J.A., Pashkevich A.V., Ronassi A.A. *et al.* Negative capacitance of nanocomposites with CoFeZr nanoparticles embedded into silica matrix. *J. Mag. Mag. Mater.* 2020. **511**. P. 166963. https://doi.org/10.1016/j.jmmm.2020.166963.
18. Sha L., Gao P., Wu T., Chen Y. Chemical Ni–C bonding in Ni–C nanotube composite by a microwave welding method and its induced high-frequency radar frequency electromagnetic wave absorption. *ACS Appl. Mater. Interfaces.* 2017. **9**, No 4. P. 40412–40419. https://doi.org/10.1021/acsami.7b07136.
19. Li J., Miao P., Chen K.-J. *et al.* Highly effective electromagnetic wave absorbing prismatic Co/C nanocomposites derived from cubic metal-organic framework. *Composites. Part B: Eng.* 2020. **182**. P. 107613. https://doi.org/10.1016/j.compositesb.2019.107613.
20. Liu X., Hao C., He L. *et al.* Yolk–Shell structured Co-C/Void/Co_9S_8 composites with a tunable cavity for ultrabroadband and efficient low-frequency microwave absorption. *Nano Res.* 2018. **11**, No 8. P. 4169–4182. https://doi.org/10.1007/s12274-018-2006-z.
21. Ebrahimi-Tazangi F., Hekmatara S.H., Seyed-Yazdi J. Remarkable microwave absorption of GO-SiO_2/Fe_3O_4 *via* an effective design and optimized composition. *J. Alloys Compd.* 2021. **854**. P. 157213. https://doi.org/10.1016/j.jallcom.2020.157213.
22. Zhao B., Shao G., Fan B., Zhao W., Zhang R. Investigation of the electromagnetic absorption properties of Ni@TiO_2 and Ni@SiO_2 composite microspheres with core–shell structure. *Phys. Chem. Chem. Phys.* 2015. **17**, No 4. P. 2531–2539. https://doi.org/10.1039/C4CP05031B.
23. Kizjak A.Yu., Evtukh A.A., Bratus O.L. *et al.* Electron transport through composite SiO_2(Si)& Fe_xO_y(Fe) thin films containing Si and Fe nanoclusters. *J. Alloys Compd.* 2022. **903**. P. 163892. https://doi.org/10.1016/j.jallcom.2022.163892.
24. Bratus' O.L., Evtukh A.A., Litvin O.S. *et al.* Structural properties of nanocomposite films SiO_2(Si) films obtained by ion-plasma sputtering and thermal annealing. *SPQEO*. 2011. **14**, No 2. P. 247–255. https://doi.org/10.15407/spqeo14.02.247.
25. Stauffer L. C-V measurement tips, tricks, and traps. *Technical report.* Keithley Instruments, Inc., 2008.
26. Mott N.F., Davis E.A. *Electron Processes in Non-Crystalline Materials*. Oxford, Clarendon Press, 1979.

Authors' contributions

Evtukh A.A.: key ideas, conceptualization, analysis, validation, conceptualization, writing – review & editing.

Kizjak A.Yu.: validation, initial draft preparation, discussion.

Antonin S.V.: writing, discussion, validation, initial draft preparation.

Bratus O.L.: investigations, discussion, key ideas.

Authors and CV

Anatoliy Evtukh defended his PhD thesis in Physics and Mathematics (Physics of Semiconductors and Dielectrics) in 1985 and Doctor of Science thesis in 2004 at the V. Lashkaryov Institute of Semiconductor Physics, NAS of Ukraine. He is Leading Researcher at the Department of Physics of Surface and Nanophotonics, the same institute. Prof. Anatoliy Evtukh has authored over 300 publications. His main research activity is in the field of nanomaterials and nanostructures, composite films with semiconductor and metal nanoinclusions, electron transport, surface physics, semiconductor technologies, sensors and solar cells.
E-mail: anatoliy.evtukh@gmail.com
https://orcid.org/0000-0003-3527-9585

Anatoliy Kizjak defended his PhD thesis in Physics and Mathematics (Physics of Semiconductors and Dielectrics) at the V. Lashkaryov Institute of Semiconductor Physics, NAS of Ukraine. He is Senior Researcher at the Department of Physics of Surface and Nanophotonics at the same institute. His main research activity is in the field of electrical properties of nanomaterials and nanostructures, composite films with semiconductor and metal nanoinclusions. E-mail: delta-epsilon@rambler.ru

Serhii Antonin, born in 1994, defended his PhD thesis in Applied Physics and Nanomaterials in 2022. Junior Researcher at the V. Lashkaryov Institute of Semiconductor Physics, NAS of Ukraine. The area of his scientific interests includes nanomaterials and nanostructures, composite films, semiconductor technologies and solar cells.
E-mail: antoninsv@gmail.com,
https://orcid.org/0000-0003-1607-9721

Oleh Bratus, born in 1981, defended his PhD thesis in Physics and Mathematics (Physics of Solid State) in 2012 at the V. Lashkaryov Institute of Semiconductor Physics, NAS of Ukraine. He is Senior Researcher at the Department of Physics of Surface and Nanophotonics at the same institute. Oleh Bratus has authored over 80 publications. His main research activity is in the field of semiconductor technologies, nanomaterials and nanostructures, composite films with semiconductor and metal nanoinclusions, electron transport, surface physics, and solar cells.
E-mail: o.l.bratus@gmail.com,
https://orcid.org/0000-0002-2661-6482

Імпеданс нанокомпозитних плівок SiO_2(Si)&Fe_xO_y(Fe), що містять нановключення Si та Fe

А.А. Євтух, А.Ю. Кизяк, С.В. Антонін, О.Л. Братусь

Анотація. У цьому дослідженні з’ясовано електричні властивості нанокомпозитних плівок, виміряні при змінному струмі. Ці плівки містять включення кремнію та заліза в аморфній матриці SiO_x. Композитні плівки SiO_2(Si)&Fe_xO_y(Fe) отримано шляхом спільного іонно-плазмового розпилення мішеней Si і Fe в кисневмісній атмосфері (Ar + O_2) з наступним температурним відпалом. Виявлено переважання індуктивного внеску над ємнісним у реактивній частині адмітансу (імпедансу) на низьких частотах (f < 1 МГц) як після відпалу в атмосфері повітря, так і азоту. Частотна залежність адмітансу після термічної обробки на повітрі має мінімуми, які зміщуються в область високих частот зі збільшенням температури відпалу. При цьому низькочастотна залежність кута зсуву фази переходить в область позитивних значень, що свідчить про переважання індуктивного внеску в адмітансі на цих частотах. Залежність дійсної частини електропровідності від частоти змінного струму істотно не змінюється до ~20 кГц. Починаючи з частоти більшої за ~20 КГц і до ~1 МГц, показник ступеня частотної залежності провідності знаходиться у межах m ~ 0,49…0,52.

Ключові слова: нанокомпозитні плівки, нанокластери Si, нановключення Fe, оксидна матриця, електричні властивості, змінний струм, імпеданс.